Ann. Rev. Biophys. Bioeng. 1977. 6:87–109

THE PURPLE MEMBRANE FROM *HALOBACTERIUM HALOBIUM*

❖9088

Richard Henderson
Medical Research Council Laboratory of Molecular Biology, Hills Road, Cambridge CB2 2QH, England

1 INTRODUCTION

Halobacterium halobium is a bacterium that occupies a special ecological niche. It can survive only in solutions containing more than 12% salt but is perfectly happy even when the salt concentration reaches saturation (1). Under conditions of oxygen starvation when the normal source of metabolic energy in the cell is cut off, *H. halobium* can use light energy. The light energy is first converted into a gradient of hydrogen ions across the cell membrane; the electrochemical gradient is then used to make ATP and, subsequently, to energize many of the normal functions of the cell.

The purple membrane, present as specialized patches integrated within the cell membrane, functions as the light-driven proton pump. It does so with only one medium-sized protein molecule and the chromophore, retinal, bound stoichiometrically. The organization of the protein:retinal complexes within each purple membrane patch is that of an exact two-dimensional crystal. Because of its intrinsic simplicity the purple membrane has become, during the last 5 years, one of the best characterized natural membranes. This review is intended to summarize the results of experiments performed during this time, to indicate some directions currently being pursued, and to show why there should soon be a deeper understanding of its structure, photochemistry, and function.

2 DISCOVERY

In 1967, as part of a careful investigation of the fragmentation products of *H. halobium,* Stoeckenius & Rowen, and later Stoeckenus & Kunau, isolated and partially characterized a purple-colored membrane fraction (2, 3). Soon after, McClare (4) also reported the separation of a distinct purple fraction from *H. halobium.* This fraction had not been observed in earlier experiments (5) with log-phase cells because it is not formed until the cells reach stationary phase (4, 6). The fragmentation of the cells, which is a convenient step in the isolation of halobac-

teria membranes, occurs spontaneously as the concentration of salt in the surrounding medium is lowered from 4.3 M (the growth concentration); the largest fragments left in distilled water are the purple membranes, which can be separated by sucrose density gradient centrifugation. After the initial discovery of the purple membrane as a separate entity, there was a lag of a year or two before other experiments characterized the membrane as a uniquely interesting and very simple system. Stoeckenius has reviewed the early history of his own and others' research on purple membrane in Scientific American (7).

Crucial experiments establishing the nature of the purple membrane were carried out in 1970. Oesterhelt & Stoeckenius (6) showed that the purple membrane contained only one polypeptide with a MW of 26,000 and that the characteristic purple color was due to retinal, vitamin A aldehyde, bound in a 1:1 ratio via a Schiff base linkage to the amino group of a lysine side chain. They named the pigmented protein bacteriorhodopsin because retinal is found elsewhere only in the visual pigments (e.g. rhodopsin). Blaurock & Stoeckenius (8) demonstrated the existence of a planar hexagonal array throughout the patches of purple membrane. The protein and probably also some of the lipid molecules in the patches are arranged in a regular and exact manner throughout the area of each patch. These observations of a simple chemical composition and a repeating physical structure established the purple membrane as a simple experimental system, amenable to several different approaches. It was not until 1973 that a definite function for the purple membrane was proposed (9, 10), i.e. a light-driven hydrogen ion pump that creates an electrochemical gradient across the membrane that can be used by the cells for ATP synthesis, along the lines of Mitchell's chemiosmotic hypothesis.

The remainder of this review gives a selective summary of some significant experiments on the purple membrane. The procedure for growing *H. halobium* and preparing purple membrane is now standard (11). Other publications reviewing the state of progress have appeared as published lectures (12, 13).

3 STRUCTURE OF THE PURPLE MEMBRANE

H. halobium is a rod-shaped bacterium (Figure 1) normally flagellated at both ends. It is an extreme halophile growing optimally in 25% (wt/vol) salt solution (1). The cell membrane is surrounded by a wall made up mainly of protein, no lipid, and small amounts of carbohydrate (3). The cell membrane, which can easily be separated from the wall proteins (3), has a characteristic dark red color; on further fractionation it can be separated into a red fraction and, in cells grown at low oxygen tension (6), a purple fraction (3). The red membrane forms by far the largest part of the membrane in well-oxygenated cells, whereas the purple membrane can account for up to 50% of the cell membrane in oxygen-starved cells. In a normal culture aerated at a fixed rate, purple membrane forms during a period of about 5 hr once the oxygen tension finally falls below a threshold level due to the increasing number of cells. The amount of purple membrane is thus controlled by the cell. If in addition to starving the cells of oxygen, strong illumination is applied, then the yield of purple membrane from the culture can be appreciably increased. It is not

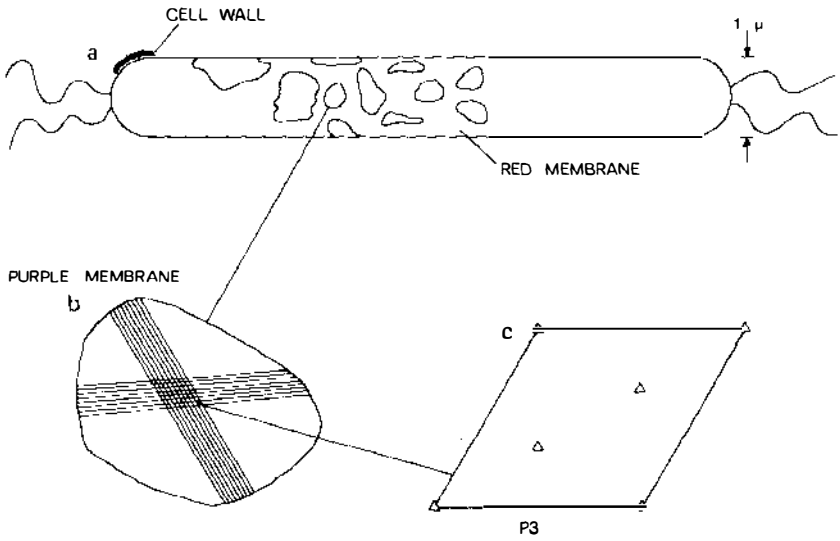

Figure 1 (*a*) Scale drawing of one *Halobacterium halobium* cell. The bacterium has flagella at both ends. A protein cell wall provides an outer coat to the cytoplasmic membrane. The membrane contains specialized purple patches to an extent dependent on growth conditions. The rest of the cell membrane is red and performs all the normal functions of the cell membrane. In the wild-type bacterium, an additional internal organelle, the gas vacuole, is present to allow the cell buoyancy. (*b*) Enlargement of a single patch of purple membrane showing the hexagonal lattice to scale. (*c*) Enlargement of one unit cell showing lattice symmetry.

clear whether the light effect corresponds to an increase in cell number, cell size, or to the fraction of membrane that is made up of purple patches; however, it is thought to be caused more by the availability of extra intracellular energy than by any additional light-induced regulation (14).

3.1 Purple Membrane is an Integral Part of the Cell Membrane of H. halobium

Freeze-fracture of intact cells (Figure 2*a*) shows that in the plane through the middle of the cell membrane there exist round or oval areas with a smoother texture, and with indications of a more regular structure than the rest of the cell membrane (8). These differentiated patches were shown (8) to be identical with the isolated purple membrane by comparing cells grown in the presence and absence of oxygen and by comparing the characteristic regular texture of the fracture faces of the differentiated purple patches with X-ray observations on the purified purple membrane fraction. The purified purple membrane (Figure 2*b*) thus was shown to exist in the cell membrane as a locally differentiated but nevertheless contiguous part of it.

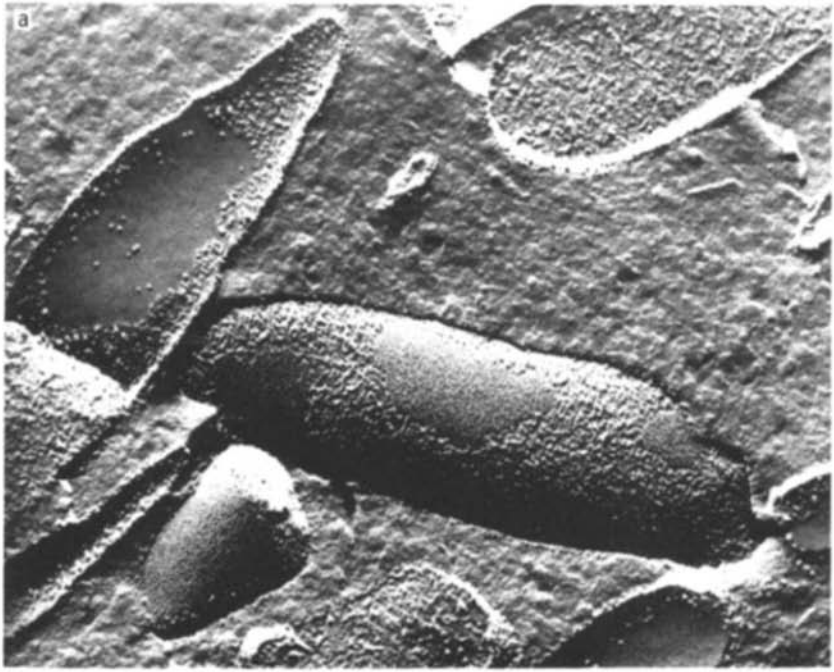
a

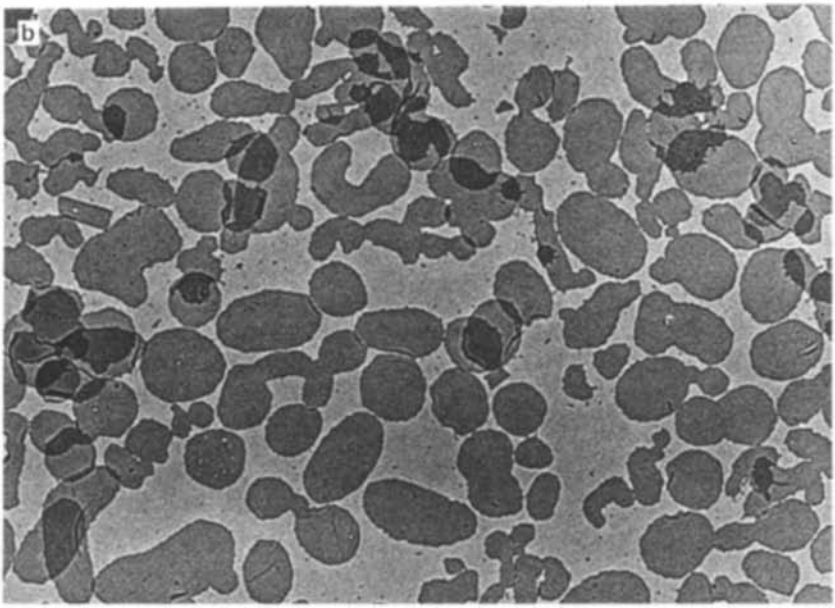
b

3.2 Purple Membrane Contains only one Polypeptide

Chemical analysis of the isolated purple membrane shows a 75% protein and 25% lipid content (6). After its solubilization in 0.1% sodium dodecyl sulfate (SDS), or 10 M urea (following extraction of lipids) and disc gel electrophoresis, all the protein migrates as a single sharp band (6) indicating that only one polypeptide is present. The MW, estimated from the mobility on the SDS-polyacrylamide gel, was 26,000 (6). Despite later demonstrations that the apparent MW on SDS-polyacrylamide gels is consistently nearer 19,000 (15, 16, 17) and that the other evidence used by Oesterhelt & Stoeckenius to confirm their 26,000 MW is now dubious (based on an out-of-date extinction coefficient for the chromophore and an amino acid analysis with low histidine content), later work has shown that the MW of 26,000 was fortuitously correct. In a preliminary investigation of the amino acid sequence by digestion with thermolysin, Bridgen & Walker (15) found six lysine-containing peptides, one of which contained two lysines, giving a total of seven. The MW from amino acid analysis, assuming seven lysine residues, is 25,100.

In contrast to the purple membrane, the red membrane contains many different protein molecules: 25 or more separate bands can be seen by SDS-polyacrylamide gel electrophoresis (Stoeckenius, personal communication) (14). It is presumed that the red membrane carries out all the normal functions of the cell membrane, whereas the purple membrane has a single specialized role.

3.3 Lipid Composition

Thorough studies of a lipid composition of purple membranes have been made on the purple membrane from *Halobacterium cutirubrum* (16). This is a closely related extreme halophile, which has also been shown to produce purple membrane (18). The purple membranes from *H. cutirubrum* and *H. halobium* are very similar if not identical (19). The lipids of the purple membrane, extracted in chloroform:methanol, contained phosphatidyl glycerophosphate (52%), phosphatidyl glycerol (4%), and several neutral lipids, largely squalenes (9%), in addition to two sulfolipid components, phosphatidylglycerosulfate (5%) and a glycolipid sulfate (10%). Triglycosyl diether (19%), another glycolipid, was also found. The sulfolipids and triglycosyl diether were not found in the red membrane fraction; instead, other unidentified glycolipids were present. The composition of the phospholipids, which form over half the total lipids, and the neutral lipids were almost identical in the red and purple fractions.

All of the lipids are thought to contain exclusively dihydrophytol chains ether linked to glycerol (20). The dihydrophytol chain is a saturated branched-chain

Figure 2 (*a*) Freeze-fracture picture of cell membrane of *H. halobium* showing patches of the purple membrane surrounded by the normal red membrane. The particles that form the purple membrane lattice are found on the cytoplasmic fracture face. (Reproduced by courtesy of W. Stoeckenius.) (X42,000.) (*b*) Typical distribution showing the sizes and shapes of purple membrane patches after purification. (X11,000.)

hydrocarbon. The role of the additional methyl groups on the otherwise straight chain may be to prevent the undesirable close packing of the lipid molecules in the membrane, a function that in other cells is performed by unsaturated fatty acids and cholesterol (20).

The red membrane also contains a number of carotenoids, which are responsible for its color, of which the chief component is the C_{50} carotenoid bacterioruberin (21). This pigment is not found in purple membrane patches. It is thought to function as a protective shield against the destructive effects of sunlight (22). The retinal chromophore in the purple membrane can also be extracted, although not completely, along with the lipids in chloroform:methanol. It is not found in the red membrane (16).

3.4 Arrangement of Protein Molecules in the Planar Hexagonal Lattice

The unusually regular arrangement of the protein and lipid components of purple membrane was first shown by Blaurock & Stoeckenius (8). They observed that the X-ray diffraction pattern of a suspension of purple membrane in water consisted of a series of sharp rings, the spacings of which arose from a two-dimensional hexagonal crystal with a 63-Å unit cell. Additional X-ray observations from an oriented sample made by drying on a flat surface (mica) showed that the hexagonal arrangement existed in the plane parallel to the membrane; the thickness of the membrane measured from the stacking distance between dried membranes was only 49 Å. The freeze-fracture experiments of Blaurock & Stoeckenius (8) (Figure 2*a*) confirmed the existence of a single, coherent, hexagonal lattice with a 63-Å cell dimension throughout each purple membrane patch. In membranes dried on freshly cleaved mica, cracks at angles of 60° to one another could also be seen in some of the membranes (8).

The calculation of how many protein molecules of MW 26,000 can be fitted into the unit cell is quite straightforward once the proportions and approximate densities of protein and lipid are known. Although values of 3.6, 3.4, and 3.3 molecules per unit cell have been obtained by using slightly different dimensions and methods of calculation (8, 23, 24) it is generally assumed that an exact hexagonal lattice can contain only whole number multiples of 3 molecules. There are therefore 3 molecules per unit cell and the packing arrangement (Figure 3) is described by the crystallographic space group P3 (23, 24). The membrane is one unit cell thick along the direction perpendicular to its plane. Other possible hexagonal space groups with 3 molecules per unit cell (e.g. $P3_1$) have symmetries inconsistent with the existence of a membrane with a precise thickness and a unique interface with the aqueous medium on each side (24).

3.5 A Predominantly α-Helical Protein

Other features found in the X-ray pattern of oriented purple membranes are striking; they concern the distribution of diffracted intensity in the pattern. It should be understood that if the purple membrane had been composed of protein and lipid molecules arranged on a hexagonal lattice, but with no other dominant feature (e.g. if the polypeptide was folded irregularly), then the atoms in the structure would be

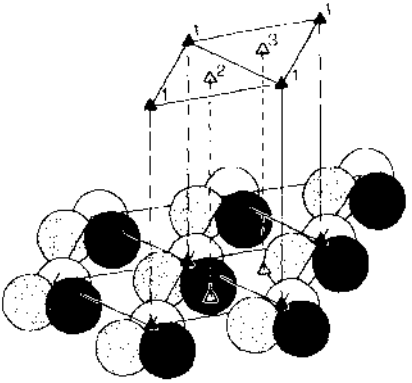

Figure 3 Diagram showing the packing of protein molecules in purple membrane. The triangles represent threefold axes relating the molecules in the lattice.

distributed rather evenly, and the diffraction pattern would be quite devoid of strong features, although it would still show the sharp lattice lines due to the crystal. Instead, very strong features are observed (8, 23, 24) at spacings of about 10 Å parallel to the plane of the membrane and at 5 Å (a broad band) perpendicular to the plane. These have been interpreted (23, 24) as arising from α-helices in the protein oriented roughly perpendicular to, and extending across, the membrane for most of its width, that is for 30–40 Å (24). The thickness of the membrane determined both from the stacking distance observed on drying (8, 23, 24) and from one-dimensional profile analysis (8, 23, 25) is in the region of 40 to 50 Å.

The 10-Å intensity in the plane of the membrane arises from the side-to-side packing of the presumed α-helices. The 5-Å intensity represents the diffraction from successive turns of the helix. An α-helix of polyalanine has a pitch of 5.4 Å and contains 3.6 residues per turn (26). The lower value observed here can be explained as arising from the tilting or possible supercoiling (27, 28) of adjacent α-helices, together with the possibility of a slightly tighter α-helix (3.5 residues per turn) than found in polyalanine. In addition, the 1.5-Å spacing that is characteristic of the α-helix (29) has been observed in dried, oriented purple membrane (23, 24); 1.5 Å is the axial distance between each amino acid residue along the helix. Thus the main features of the diffraction pattern suggest a structure for the protein that is composed largely of α-helices arranged perpendicular to the plane of the membrane and extending across it for most of its width. Unpublished CD measurements in the 208–222 nM region, which is diagnostic of secondary structure in proteins, have also indicated 60–70% α-helix in sonicated purple membrane fragments (Stoeckenius, personal communication).

Other less pronounced features of the X-ray pattern exist; for example, there is an enhanced intensity at 4.6 Å parallel to the plane of the membrane. This probably arises from the alignment of the lipid hydrocarbon chains in a direction perpendicular to the plane of the membrane and separated by approximately 4.6 Å (23, 24), as found in other membranes.

3.6 Three-dimensional Model Obtained by Electron Microscopy

By exposing purple membranes to electron doses sufficiently low to avoid the complete destruction of their intrinsic structure, Unwin & Henderson (30) were able to record electron diffraction patterns and electron images that displayed the hexagonal lattice structure of unstained purple membrane. Using 15 to 20 electron diffraction patterns and micrographs of membranes tilted at different angles to the incident beam of electrons, the amplitudes and phases of the Fourier components needed to define the structure of the membrane in three dimensions were obtained (31). A model (Figure 4) derived in this way, corresponding to the part of the membrane containing one molecule of the protein bacteriorhodopsin, shows several interesting features. There are seven rods about 40 Å long and 10 Å apart that extend across the membrane roughly perpendicular to its plane. These are presumed to be α-helices. There are three (at the back in Figure 4) almost exactly perpendicular to the plane of the membrane and four (at the front in Figure 4) progressively more tilted at angles from 10° to 20° to the plane of the membrane. The lipid molecules have been drawn (Figure 4) to occupy their likely but not yet proven positions. Neither the position of the retinal nor the orientation of the purple membrane model in the cell membrane (that is, which side of the cell membrane corresponds to "up" in the model) is yet known. Hopefully, specific labeling of the retinal site and the inside (or outside) of the membrane will eventually be possible and will provide answers to these questions.

3.7 Rotational Mobility

Experiments similar to those first used (32) to measure the rotational mobility of rhodopsin in the disc membranes of rod outer segments from frog retina have also

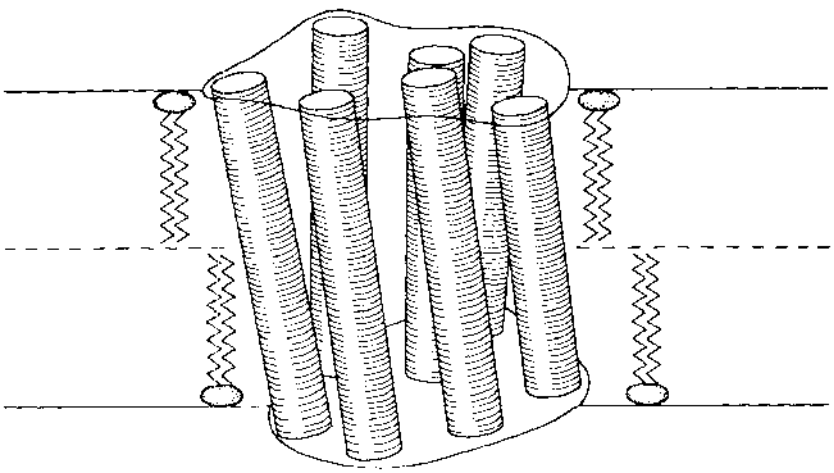

Figure 4 Drawing showing the arrangement of α-helices in one protein molecule of the purple membrane, derived from electron microscopy (31). The lipid has been drawn to occupy its likely but not yet proven position. The position of the retinal chromophore is not known.

been carried out on purple membrane (33, 34, 35). In these experiments, the lifetime of the dichroism induced by bleaching the chromophore with a flash of polarized light is measured. Not surprisingly, rotational motion was found to be very slow. The observed half-life of 70 msec (34) agrees well with that expected (35) theoretically for patches with a diameter of 0.5 μm that behave as rigid bodies. The forces between the protein molecules making up the lattice seem to be strong enough to prevent any rotations within the lattice, in addition to holding the crystal together.

4 PHOTOCHEMISTRY

Because of the similarity of the photochemical reactions of retinal in the purple membrane protein bacteriorhodopsin to those in rhodopsin, the visual pigment in the eye, many of the techniques already used to investigate rhodopsin have been successfully and quickly applied to purple membrane. In addition, there are several experiments that do not work with the visual pigments but that have produced quite clear-cut results when applied to the purple membrane. Use of the name bacteriorhodopsin for the purple membrane protein allows the term bacterio-opsin to be used when discussing the protein from which retinal has been removed, again by analogy to the opsin-rhodopsin terminology.

4.1 Identifying Retinal as the Chromophore: Attachment to a Lysine Residue

Oesterhelt & Stoeckenius (6) applied a number of spectroscopic and chromatographic techniques to the extracted chromophore and its derivatives (retinol and retinaloxime). These tests proved that the purple membrane chromophore was retinal (Figure 5) and excluded, for example, dehydroretinal. The tests included high-resolution mass spectrometry of the reduced chromophore (retinol), indicating the empirical formula $C_{20}H_{30}O$, and observation of the specific color reaction with antimony trichloride. In addition, the retinal was found to be attached to the protein via a Schiff base to the ϵ-amino group of a lysine residue (6). The sequence of amino acids around this lysine (*) has been determined as Gly-Val-Ser-Asp-Pro-Asp-Lys-Lys(*)-Phe-Tyr-Ala-Ile-Met (15). Careful examination of the nature of this sequence shows that there are six adjacent hydrophilic amino acids, including a proline, flanked by exclusively hydrophobic residues. It is probable that this sequence forms one of the connecting links between the ends of two of the α-helices in the model, and therefore that the retinal is positioned close to one of the membrane surfaces (15).

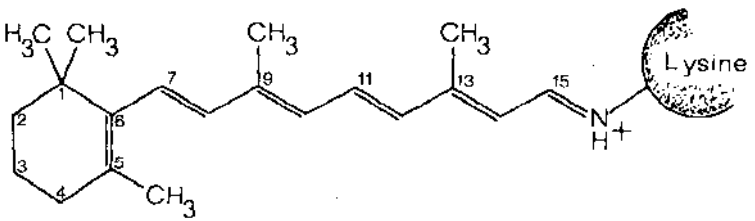

Figure 5 The chromophore, all-*trans* retinal. In the membrane it is attached via a Schiff base to the ϵ-amino group of one of the seven lysine residues.

4.2 Retinal Isomers Obtained by Extraction and Required in Reconstitution

The retinal can be extracted into petroleum ether at 40–60°C after a suspension of the purple membrane in water is treated with a solution of the detergent cetyltrimethylammonium bromide (CTAB) or dimethylsulfoxide (Me_2SO), followed by acetic acid (6, 36). Subsequently, thin-layer chromatography in dim red light reveals that the isomer of retinal present in membranes that are light-adapted (see next section) is exclusively all-*trans*, whereas an appreciable amount (almost half) is extractable as the 13-*cis* isomer in membranes that have been kept in the dark. This identification has been confirmed (36) by extracting the retinaloxime derivatives formed by treating the membranes with hydroxylamine instead of acetic acid, and subsequently identifying the 13-*cis* and all-*trans* isomers by thin-layer chromatography. A report that the dark-adapted isomer is not a mixture of 13-*cis* and all-*trans* but is exclusively 13-*cis* (37) may be due to the use of only partial and selective extraction (yield ~20%) of the chromophore into chloroform at 0°C. More efficient extraction into ethanol at O°C (38) or dichloromethane (Pettei et al, personal communication) has confirmed the presence of approximately equal amounts of 13-*cis* and all-*trans* isomers in the dark-adapted membranes.

An interesting feature of the analysis of the products formed from the hydroxylamine reaction (36) is that the two possible stereoisomers that can be produced, the syn and anti forms, are not produced in equal amounts in membrane treated with Me_2SO in the dark. Only one 13-*cis* and one all-*trans* isomer are produced. There is no doubt that the reaction of the –C=N– double bond of the Schiff base with hydroxylamine in 50% Me_2SO is a stereospecific reaction. By contrast, the reaction of hydroxylamine with purple membrane in CTAB, or during illumination, either with or without Me_2SO, gives rise to both syn and anti isomers (36). These observations reflect changes at the atomic level in the conformation of the protein or the retinal, or both, near the Schiff base during illumination. Indeed, the absence of a measurable reaction with hydroxylamine in the dark (36) without Me_2SO indicates that the Schiff base is in some sense inaccessible to small reagents until illuminated. However, as this could be due to the stronger protonation of the Schiff base in the dark, it is not such a firm indication of a change of conformation at the Schiff base as is the alteration by light of the retinaloxime isomers produced in membranes suspended in Me_2SO solution.

Apomembrane can be made (36, 39) by treating the purple membrane with hydroxylamine under strong illumination. The apomembrane is colorless (the retinaloxine absorbs at around 360 nM); adding retinal to the apomembrane regenerates the characteristic purple complex (40). Different isomers of retinal, however, regenerate at different rates. 13-*cis* retinal is faster than all-*trans* retinal and initially they give slightly different absorption spectra. Eventually, however, as the dark equilibrium of isomeric forms is attained, the visible absorption spectra from membrane regenerated with either 13-*cis* or all-*trans* retinal become identical. Neither 11-*cis* nor 9-*cis* retinal will regenerate the purple color (40). The behavior in regeneration experiments thus is a wholly independent indication of the isomeric state of the retinal in the purple membrane.

4.3 Kinetic Analysis of Intermediates by Flash Spectroscopy

Since even in strong sunlight a suspension of purple membrane does not visibly change its color, the light reactions that occur must be investigated spectroscopically, either by using very intense light flashes or by perturbing the kinetics of the photochemical cycle. The second method is simpler and provided the first evidence for the reaction cycle. At this point, the slow equilibrium between light-adapted and dark-adapted membrane should be explained in more detail. Membrane exposed to light absorbs at 570 nM and contains all-*trans* retinal. Membrane subsequently kept in the dark gradually ($t_{½} \simeq 20$ min at 35°C) changes to a form absorbing at 560 nM and containing a mixture of all-*trans* and 13-*cis* retinal (6, 36). This slow equilibrium, which takes place in the dark, may not have any biological function since it may be more a reflection of the flexibility that the protein allows the retinal in the region of the 13-*cis* bond. In any case, the light-adapted form is undoubtedly the form that exists under physiological conditions and to which most of the experiments pertain.

Oesterhelt & Hess (41) initially measured the bleaching, by light, of the purple complex of bacteriorhodopsin (bR_{570}) into a compound absorbing maximally at 412 nM, by using suspensions of purple membrane in concentrated salt solution saturated with diethylether. The purple complex reappeared in the dark with a half time of 13 sec at 20°C. The effect of the ether was to slow down the 412 $\longrightarrow$ 570 dark reaction, by a factor of about 1000, so that it could be observed easily. In addition, they observed a release of protons concomitant with the formation of the 412 complex and an equal uptake on regeneration of the 570 complex. The 412 complex can also be trapped without using ether by cooling a suspension of membranes during illumination (9, 42, 43). On warming this bleached, frozen specimen, the 570 complex reappears. These simple demonstrations of the occurrence of a photochemical cycle have now been supplemented by extensive results from flash spectroscopy in the absence of organic solvents.

The most complete analysis so far is that by Lozier et al (34, 42, 44); it is their terminology and conclusions that are presented in Figure 6. Results in substantial agreement with those of Lozier et al have also been published by others (17, 35, 45, 46, 47). The experiments have been carried out mainly on the light-adapted bR_{570} form of the membrane (44); however, it is believed (17, 44) that the dark-adapted bR_{560} form of the membrane, or that part of it containing 13-*cis* retinal, undergoes a similar cycle.

At −196°C, bR_{570} can be converted into a roughly equal mixture of itself and a red-shifted photoproduct K_{610} by illumination with 500 nM light (34, 44). Subsequent illumination with 650 nM light completely regenerates bR_{570}. Apparently, the absorption spectra of bR_{570} and K_{610} overlap at shorter but not longer wavelengths so that a photostationary equilibrium is obtained, with a maximal proportion, depending on the illuminating wavelength, of about 50% in the 610 form. The K_{610} complex resembles prelumirhodopsin in its red shift and in its ability to be produced photoreversibly at −196°C. When the mixture of bR_{570} and K_{610} is warmed slowly in the dark, the K_{610} complex decays through two more intermediates, termed L_{550} and M_{415}, before regenerating the initial bR_{570} purple complex (Figure

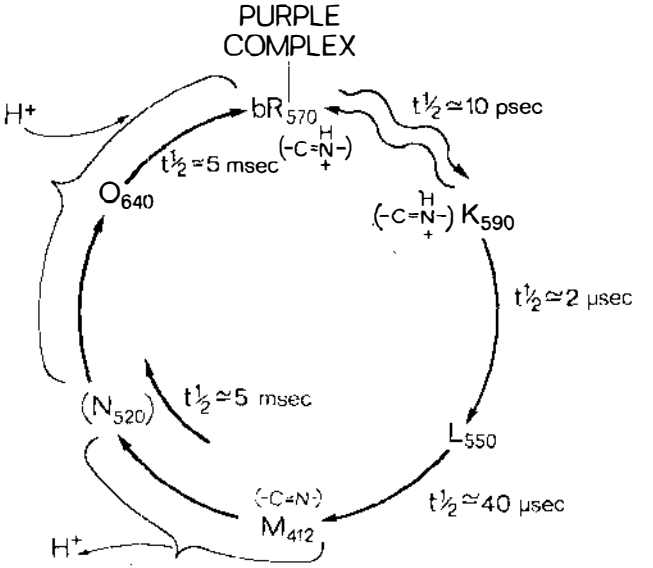

Figure 6 A current model showing the intermediates detected in the photochemical cycle of the purple membrane by low temperature and flash spectroscopy (44). One hydrogen ion is released and taken up again, near the positions shown. The protonation states of the chromophore are also shown. They are derived by resonance Raman spectroscopy. A similar series of intermediates is well known in the visual pigment, rhodopsin, which also contains the chromophore retinal, in a 1:1 complex with the protein.

6). Intermediate M is the one that can be trapped in the salt-ether system and by cooling to −196°C during illumination. The transition bR ⟶ K is the only light-driven reaction, all others following in the dark, driven by thermal energy.

Flash spectroscopy at 1°C indicates that the same intermediates K, L, and M occur at near physiological temperature with slightly different absorption maxima (K_{590}, L_{550}, M_{412}). Their absorption spectra have been calculated (34, 44) from the transient changes observed at different wavelengths after a brief laser flash. A further intermediate, O_{640}, is observed in experiments at 40°C (17, 35, 44), but not at 0°C because of the temperature dependence of the rate constants. Finally, an intermediate N_{520} is suspected because the spectrum derived for M seems to vary with the temperature of the experiment (34, 44). Figure 6 gives a summary of the present best scheme for the photochemical cycle, with the approximate half-lives of each intermediate at room temperature indicated. The half-time for formation of the first intermediate, K_{590}, required special picosecond measurements (48) that show its appearance with a half-time of about 10 psec. Finally, there is every probability (34, 35) that the scheme depicted in Figure 6 will need some modification once the effects of pH, temperature, and possibly one or two solvents on the kinetics of the cycle have been fully investigated. So far, there is no evidence for any kinetic coupling

between neighboring molecules in the lattice; no suggestion of cooperativity has been found.

The release and uptake of protons, first observed in the salt-ether system (41) with a glass electrode, can also be measured spectrophotometrically in the absence of ether by using a pH indicator dye. When this is done (44, 49) at 21°C, it appears that one proton is transiently released for each molecule of pigment cycling; the release occurs at or just following M and the subsequent uptake somewhere in the N $\longrightarrow$ R sequence (44, 49). The proton release also correlates with the formation of M_{412} at –40°C (45). Oesterhelt has further stated, from steady-state measurement of the amount of 412 complex formed at high light intensity, that approximately one proton is released for every 412 complex formed (43).

It is believed that the proton released from isolated purple membrane sheets is released from the external surface of the membrane and that subsequent uptake is on the cytoplasmic surface. Very recent experiments with reconstituted vesicles and cell envelopes, in which the purple membranes have, respectively, the cytoplasmic surface and the external surface oriented preferentially to the outside, have experimentally demonstrated that this does indeed occur (49). The vesicles showed a net alkalinization in the 10-msec time range, whereas the envelopes showed a net acidification with a half-time of less than 1 msec.

4.4 Resonance Raman and Fluorescence Spectroscopy: Retinal Conformation

The extraction of a particular isomer by organic solvents, such as all-*trans* retinal from light-adapted purple membrane, suggests that the retinal has a conformation close to all-*trans* when bound to the protein. What, then, do the five or six distinct intermediates observed by low temperature or flash spectroscopy represent? What causes the absorption maximum of bR_{570} to be red-shifted from the normal position observed for a Schiff base between, for example, retinal and hexylamine in methanol? What does the absorbed light energy do to the retinal-protein complex that allows some of the energy to be stored during the photochemical cycle and part of that to be used to pump protons across the cell membrane? Clearly, the answers to these questions will come from a knowledge of the structure of the retinal-protein complex and the sequence of conformational changes that follow the absorption of light. These changes in conformation will presumably include changes in the positions of the atoms in retinal. However, the detail necessary to see individual atoms is unlikely to come from diffraction methods. The best that can be hoped for is that the environment of the retinal (amino acid side chains, charged groups) will be determined. Although this would be very valuable, more detailed questions about the conformation of the retinal will remain. In particular, the determination of the conformation about the single bonds and thus of any deviation from the planar configuration normally found for polyenes will be more difficult.

Resonance Raman spectroscopy of the purple membrane and its photochemical intermediates (50, 51, 52) offers an experimental approach to analysis of the retinal conformation. The resonance Raman method displays the frequency spectrum of the vibrational modes of the absorbing chromophore as indicated in the energy-loss

spectrum of Raman scattered light. The spectrum is similar to the infra-red absorption spectrum of the compound being analyzed but contains only minute contributions from parts of the structure (such as the protein in this case) not directly conjugated to the chromophore. A complete analysis of the resonance Raman spectrum would entail calculating the expected vibrational modes from a model and correlating them with the observed peaks. Hopefully, the spectrum is rich enough in detail to be uniquely interpretable in terms of the retinal conformation.

So far, only a few assignments of peaks in the spectrum have been made, but these have already proved extremely valuable. Lewis et al (50) have shown, by analysis of the –C=N– stretching frequencies in D_2O and H_2O, that in the purple membrane complex bR_{570} the Schiff base retinylidene-lysine linkage is protonated and that in the M_{412} complex it is unprotonated. More recently (53) the first intermediate, K_{590}, has also been shown to be protonated. The flash spectroscopic result showing that the release of a proton into solution is most closely correlated in time with the formation of M_{412} is in good agreement with this. The two sets of data taken together suggest that the Schiff base may be directly involved in the proton release (and uptake), although the exact timing and whether other groups on the protein are involved is not completely clear. Some other assignments in the resonance Raman spectra have been made (52, 54) by comparison with retinylidene-lysine compounds. They provide information on the extent of C=C double bond formation and electron delocalization out of the polyene system in the different photochemical intermediates. The causes of the change in protonation state of the Schiff base and the lowered C–C bond order, however, remain unknown. The detailed conformation of the retinal and the positions of surrounding side chains in the protein is still substantially unknown.

The observation of fluorescent light emission (54–56) from the chromophore in purple membrane is expected to provide some information about the character of an excited state that is produced before the K_{590} intermediate, presumably the excited state from which K_{590} is formed. Picosecond absorption measurements (48) have also suggested the existence of a transient intermediate between bR_{570} and K_{590}. Further investigation of these very early events after absorption of a photon should help in understanding the origin of the red shift in the retinal-protein complex and the mechanism of light energy storage and eventual conversion into a hydrogen ion gradient.

4.5 Visible Circular and Linear Dichroism: Interaction Between Chromophores of Different Molecules and Retinal Orientation

The existence of intense positive and negative bands in the visible CD spectrum of purple membrane (57, 58, 59) results from the coupling between retinal chromophores in adjacent molecules in the lattice. The bands are centered at the absorption maximum of the chromophore at 570 nM; the coupling is due to the formation of an exciton dimer or multimer between neighboring chromophores. In this case, because of the threefold axes, a trimer is more likely to be the structure responsible (58). The positive and negative bands from the exciton coupling are superimposed on and centered at the position of the more normal positive CD band due to the

interaction of the retinal with the asymmetric protein binding site. The positive CD band can be observed separately in molecules solubilized in individual detergent micelles (57, 59) or by partial (~10%) reconstitution of apomembrane, so that most of the retinal does not have a near neighbor (58, 59). The strong exciton coupling is possible because the retinal sites in adjacent molecules are physically close, the dielectric constant within the membrane is low, and the extinction coefficient of the chromophore is high (58). The magnitude of the exciton coupling is determined by the geometrical relationship between the transition dipoles of the retinal and the inter-retinal vectors. Hence, if the distance between the retinal molecules is known, information about their orientation can be deduced. Already it can be stated (58, 59) that the transition dipole of the retinal cannot be exactly in the plane of the membrane because then there would be zero exciton coupling.

The measurement of linear dichroism at 570 nM in oriented specimens by Blaurock & Stoeckenius (8) showed that the long axis of the retinal was more closely parallel to the plane of the membrane than perpendicular. The visible band CD measurements show that it cannot be aligned exactly parallel to the membrane. More accurate linear dichroism measurements on oriented specimens together with a more detailed interpretation of the CD spectrum may determine the retinal orientation more precisely. A recent kinetic study (34) of the linear dichroism induced by a flash of polarized light showed a small component with a half-life of about 0.3 msec, which was taken to provide the first evidence of a change in orientation of the retinal during the reaction cycle.

4.6 Theoretical Models for the Photochemical Events

The events that follow absorption of a photon by the retinal-protein complex in the purple membrane, and more especially in rhodopsin, the visual pigment, have been the subject of much debate, controversy, and speculation. Reviews and articles that might be referred to on the state of play have been included as references (60–66).

5 FUNCTION AS A PROTON PUMP COUPLED TO ATP SYNTHESIS

Purple membrane is thought to function as an electrogenic hydrogen ion pump driven by light. Protons are pumped out of the cell. The electrochemical gradient of hydrogen ions is then used to synthesize ATP, as proposed by Mitchell (67, 68) for energy coupling in chloroplasts and mitochondria. This section of the review discusses the experiments on which this conclusion is based.

Oesterhelt & Stoeckenius (9) first postulated that the purple membrane functioned as a light-energy convertor on the basis of the following observations:

(*a*) cells synthesize purple membrane when their normal supply of metabolic energy is interrupted [that is, during a shortage of oxygen and when provided with light (6, 9)];

(*b*) protons are released from purple membrane sheets when bleached to the 412 form (9, 41);

(*c*) light reduces the pH of suspensions of cells containing purple membrane (9, 10), and uncoupler abolish the effect;
(*d*) oxygen consumption by respiring cells is reduced by light if the cells contain purple membrane (9, 69).

Further support for their proposed function came from later experiments showing light-driven ATP synthesis (12, 70), light-driven increases in the pH gradient and electrical potential across the membranes of cells (71, 72) and resealed envelopes (73), and lastly from experiments in which light-induced pH differences and membrane potentials were produced between the two sides of artificial vesicles (74, 75) and black lipid films (76) containing only the purified purple membrane patches.

The action spectra of the light-induced pH changes (78, 79), the inhibition of respiration (69), ATP synthesis (70), and a phototactic response that keeps the bacteria in the brightest part of an illuminated field (77) all follow the absorption spectrum of isolated purple membrane. This shows that all of these effects are mediated by the initial absorption of light by the chromophore.

The function of the bacteriorhodopsin as a light-driven proton pump therefore seems to be proven beyond doubt. However, calculating the efficiency of converting the light energy into an electrochemical H^+-ion gradient suggests that a considerable amount of the available light energy is lost. Each absorbed photon (energy 2 eV or 45 kcal/mole) translocates 0.5 to 0.8 (12, 13, 72, 78, 79) protons across the cell membrane against an electrochemical potential [proton motive force (pmf)] of 180 to 280 mV (71, 72, 73, 76), which gives an overall efficiency for this step of 5 to 10%. Conceivably, the remaining 90 to 95% of the incident light energy is simply lost as heat, but it should not be forgotten.

5.1 Experiments on Intact Bacteria and Resealed Cell Envelopes

Quite separate from those observations that support the proposed function of the purple membrane are a number of more detailed observations of considerable interest. Not all of the observations have an agreed interpretation.

Measurements of the reduction in oxygen consumption by light (69) show that the absorption of around 24 photons by the purple membrane in halobacteria is required to reduce oxygen consumption by one molecule. The quantum efficiency for the photochemical cycle has been variously estimated at between 0.5 (34) and 0.8 (41) and the number of protons translocated is estimated at approximately one per molecule of protein cycling (43, 44, 49). Thus, approximately 0.6 to 0.7 protons are translocated per photon absorbed (72, 79). Since the oxidation of substrate by one oxygen molecule is thought to give rise to at least six (possibly eight) molecules of ATP via 12 (or possibly 16) protons translocated (80), it is clear that the observed light inhibition of respiration and proton pumping stoichiometry are in excellent agreement with existing numerology.

There is also substantial agreement on the pH gradients and membrane potentials that exist in both dark and light anaerobic cells. Apparently, even in cells kept for long periods anaerobically in the dark, an appreciable electrochemical hydrogen ion gradient is maintained by some unknown energy source. Addition of CCCP (carbonylcyanide *meta*-chlorophenylhydrazone) or other uncouplers that increase the

permeability of membranes to protons produces net alkalinization of the medium in the dark (9, 12, 81). Both the magnitude of the pH gradient (ΔpH) and the membrane potential ($\Delta\psi$) in cells and resealed envelopes have been estimated using lipophilic ions (71, 72) or fluorescent probes (73, 72) and various buffers. For cells kept anaerobically in the dark, a total pmf consisting of both ΔpH and $\Delta\psi$ components of 130 to 150 mV was estimated (71, 72, 73), rising by a further 20 to 30 mV when the light is on. Blocking the ATP synthesizing enzyme with the specific reagent DCCD (dicyclohexylcarbodiimide) allowed pmf values as high as 280 mV to be produced by light (71). Thus the electrochemical gradient appears to be of the right size for its proposed function and can be induced by light in cell envelopes (73) devoid of intracellular proteins. The origin of the pre-existing gradient present in dark, anaerobic cells may be concerned with the equilibration of other ionic species across the cell membrane. The concentrations of potassium ion (high inside, low outside) across the cell membrane (82) together with the suspected greater permeability to potassium than to other ions (81) suggest that the membrane potential may be simply the potassium equilibrium potential. The potassium ion gradient represents a considerable store of energy for the cell, which can be maintained for long periods (82), possibly because of very low permeability to other ions.

The interpretation of changes in the pH of cell suspensions during illumination has involved some differences of opinion that will only be resolved by future experiments. When cells kept anaerobically are illuminated, there is generally an initial alkalinization of the medium followed by a slower acidification (9). The extent of both of these effects varies somewhat depending on the light intensity, the pH of the suspension, and the length of time the cells have been kept anaerobically in the dark, but generally for repeated illumination with strong light at pH 6-7, the final net acidification of the medium is the larger effect. Both the alkaline transient and the final acidification are optimally produced by 570 nM light. Regardless of the shape of the pH changes on illumination, ATP levels always increase and reach an equilibrium level at about the time when the alkaline transient is completed. Thus, the alkalinization is correlated kinetically with ATP synthesis (12, 43, 72, 81). If the ATP synthetase is blocked with DCCD then the alkaline transient is also abolished and only a large acidification is observed (12, 81). It is clear that this acidification, and that in cells untreated with DCCD, is due to the light-driven proton extrusion. However, so few protons can be pumped out electrogenically (i.e. without compensating charges) before the membrane potential reaches an unrealistically high value (Oesterhelt has calculated that $\sim 4 \times 10^4$ protons per cell would give a 300-mV potential), and this would occur in times of about 1 msec for a typical cell (12, 43), that the large acidification can only occur if other ions are allowed to move to provide an electroneutral exchange. For outward proton movement sufficient to produce observable pH changes, a compensating inward movement of, for example, potassium ion would be required. These movements are slow and occur over time scales of seconds to minutes.

The production of ATP from an electrochemical hydrogen ion gradient must also involve the transfer of protons without compensating charges for the electrical part of the pmf to be used. Since all measured changes in pH have to be caused by

electroneutral processes, we must look to these to explain the initial alkalinization. Oesterhelt (12, 13, 43) has suggested one reasonable explanation: the consumption of up to one proton by the reaction ADP + Pi $\longrightarrow$ ATP, which is expected to occur (above pH 6) due to the differences in ionizable groups between starting material and products. The increased pH inside the cell would increase the pmf and pull in protons from the outside causing an alkalinization of the medium. It is not known whether the internal buffering capacity of the cell is small enough to allow for this magnitude of pH change. Neither does this qualitative explanation, implying a net removal of up to one proton per molecule of ATP formed, apparently agree with the magnitude of the alkalinization effect. Bogomolni et al (81) have quantitatively measured a ratio greater than 2 H^+/ATP molecule during the initial alkalinization, and Oesterhelt et al (43) have shown that a quadrupling of the light intensity causes a much faster and larger alkalinization without any corresponding change in the rate or extent of ATP formation. Thus, other processes seem to be occurring (43, 81). Whether this reflects the coupling of the light-induced hydrogen ion gradient to other physical or chemical reactions in the cell's metabolism will not be known until further experiments are carried out.

Bogomolni et al (81) have suggested that the alkaline transient, which they measure as about 2.9 H^+ ions/ATP, simply represents the protons required by the ATP synthetase and that they are driven by the pre-existing membrane potential arising mainly from the potassium gradient. They postulate that the ATP synthesis is triggered by the pmf (or pH gradient or internal pH), with a delay of a few seconds after switching on the light, through the dissociation of an inhibitory subunit from the ATP synthetase. Recombination of the inhibitory subunit switches off the enzyme, again with a few seconds delay, when the light is removed. This explanation involves the rather tricky assumptions of hysteresis in the activation and deactivation of the ATP synthetases and a spread in the triggering sensitivity of different molecules (81). It seems more likely that another explanation will be found, still involving perhaps the release and uptake of an inhibitory subunit but without the need for these assumptions. Experimentally, it may be necessary to measure, simultaneously, the number of photons absorbed, the cycling efficiency, and the pH and membrane potential, as well as the levels of ATP and other cellular reactants. Such measurements, although difficult, are already being tackled (72, 79).

5.2 Experiments with Artificially Made Vesicles

Using a cell-free system with defined constituents, the results of experiments are often more easily and less ambiguously interpreted. It is significant therefore that Racker & Stoeckenius (74) showed that purple membrane could be incorporated into vesicles that produced a measurable uptake of protons in the light. By including the mitochondrial oligomycin-sensitive ATPase during formation of the vesicles, a degree of light-sensitive phosphorylation was obtained (74). Although only a maximum of between one and four protons per molecule of pigment was taken up by the vesicles, it was nevertheless sufficient to prove a pumping role for the purified purple membrane. Note also that the direction of proton translocation was the

opposite of that found in whole cells, showing that the membranes were incorporated preferentially inside out, a result confirmed by freeze-fracture (49). Similar experiments with purple membrane vesicles have been carried out that demonstrate the electrogenic nature of the proton pumping (75, 83) and that use a more stable ATPase preparation (84) from a thermophilic bacteria. Other methods of making vesicles have produced larger maximal pH changes; the largest response reported so far after reaching a steady state in the light is 34 protons per molecule of bacteriorhodopsin (85).

5.3 Electrical Measurements on Membranes Incorporated into Black Lipid Films

Purple membrane can be incorporated into Mueller-Rudin black lipid films separating two aqueous compartments either by incorporation from the aqueous phase as vesicles (76) or by inclusion in the decane solution used to form the black lipid film (86). In the light, potentials of 20–150 mV are measured between the two compartments. With the incorporation from vesicles the compartment to which the vesicles were added became negative, whereas with the inclusion in decane the magnitude and sign of the effect varied, presumably depending on the fortuitous orientation of the membranes. The largest potentials were produced by 570 nM light as expected for purple membrane (86). Measurement of the maximal emf (measured from the equal and opposite applied voltage required to reduce the observed current to zero) showed values as high as 300 mV (76), a number that correlates well with estimates for the performance of purple membrane in intact cells blocked by DCCD (71).

5.4 Observation of Phototactic Response

Phototaxis in *Halobacterium halobium* has been studied by Hildebrand & Dencher (77). The effect observed is phobic—the bacterium stops swimming and after a small delay starts again in the opposite direction. Two types of response were observed: one response to a reduction in light intensity has an action spectrum centered at 565 nM; a second response to increased light intensity has an action spectrum with several peaks in the ultraviolet to blue region. The presumed function of these responses is to maintain the bacterium in the brightest part of an illuminated field so that the light energy can be used to maintain the cellular ATP levels, but to avoid regions of strong ultraviolet radiation that would damage the DNA.

The peak at 565 nM in the action spectrum of the first response, together with its low sensitivity (77), suggests that it is mediated via the purple membrane, in all probability through the hydrogen ion gradient. So far we have very little idea of how either the initial light absorption or the proton gradient, is coupled to the bacterial motion. However, an excellent review of chemotaxis in bacteria is available (87) that discusses what is known about coupling. Presumably similar principles will apply in the coupling to bacterial motion of the signals from both chemical receptors and photoreceptors.

6 BIOSYNTHESIS AND ASSEMBLY

The best study of purple membrane biosynthesis is that of Sumper et al (14). They followed the synthesis of (*a*) retinal and its presumed precursors lycopene and β-carotene, (*b*) the protein of purple membrane, bacterio-opsin, and (*c*) the lipids. They found that the conditions of low oxygen tension and high light intensity that were found optimal for purple membrane production (9, 11) did not have much effect on lipid synthesis; that is, the lipids in purple membrane were formed during growth well before the protein or the retinal. Both the appearance of the protein and the retinal were triggered by lack of oxygen. Cells with a sufficient supply of oxygen contained only 10 to 20% of the normal amount of retinal but high levels of lycopene. Conversely, optimal production of retinal (in purple membrane) led to low concentrations of lycopene. The ratio of β-carotene to retinal did not seem to change much. Hence, the regulation of purple membrane production seems to be at the level of lycopene to β-carotene conversion for the chromophore and at the level of gene expression for the bacterio-opsin (14). Regulation seems to be triggered by inadequate levels of oxidative phosphorylation. The additional presence of light does not seem qualitatively to affect the regulation of purple membrane production, but it may speed up its production by providing an additional energy source to make the ATP necessary for protein synthesis.

It is not known how the protein in purple membrane is incorporated into the cell membrane after its synthesis on the ribosome. However, once incorporated as individual polypeptide chains, it is believed to form the two-dimensional crystalline patches by a process of self-aggregation or two-dimensional crystallization. The belief is based on two observations. The first is that purple membrane can be solubilized in Triton X-100 (2 g of detergent per g of purple membrane; Henderson, unpublished experiment) at pH 5 and 20°C to give a stable, clear solution of protein:lipid:detergent micelles containing protein monomers. Subsequent removal of the detergent by extensive dialysis and washing allows the membrane to reform as very large but nevertheless crystalline vesicles. This experiment proves that the ability to assemble into crystalline patches is a property of the bacteriorhodopsin molecule in the appropriate lipid environment. The second observation is that the apomembrane, formed by bleaching with hydroxylamine (39), has lost its crystallinity; if the bleaching is carried out in whole cells a gross decrease in the density of the membrane fraction containing bacterio-opsin occurs, producing isoapomembrane (39) with a much more loosely packed, noncrystalline arrangement of protein. Reconstituting the pigment by adding back retinal causes recrystallization of the protein into the same hexagonal lattice in both apo- and isoapomembrane (Henderson and Oesterhelt, unpublished observations). Again, it is clear that bacteriorhodopsin spontaneously forms two-dimensional crystals.

The effect of metabolic blockage of retinal synthesis on the formation of purple membrane (14) is therefore of special interest. Nicotine (1 mM) inhibits the cyclization of lycopene to β-carotene (88). Halobacteria grown in the presence of nicotine, therefore, accumulate lycopene at the expense of retinal and β-carotene, but they continue to produce the protein bacterio-opsin (14). The experiments with hydrox-

ylamine on whole cells would lead us to expect that the bacterio-opsin (in cells grown in the presence of nicotine) would occur in membranes with a density similar to that of isoapomembrane. This indeed occurs. A fraction containing all the bacterio-opsin is found at about the same density as isoapomembrane (14). It has been termed brown membrane, because it also contains some material absorbing at 419 nM (cytochrome). When retinal is added to this brown membrane fraction, the characteristic 570 nM band of bacteriorhodopsin is regenerated, but the lattice does not reform (14). It is not known why the lattice does not appear spontaneously, and therefore some modification of the protein is suspected. If retinal is added to the nicotine-treated cells prior to isolation of the membrane fractions, the crystalline purple patches are formed if the cells are allowed to metabolize, but only the noncrystalline membranes of lower density are found if the cells are kept anaerobically in the dark. An ATP-dependent modification of the membrane is therefore suspected (14).

Thus the synthesis of retinal and the protein in purple membrane are separately induced by low oxygen tension, but the molecular mechanism of the induction is unknown.

7 CONCLUSION

The purple membrane is a very simple system that hopefully will provide the answers to a number of basic biophysical questions. It forms a crystalline array containing only one protein of about 26,000 MW, from which detailed structural information about the folding of a membrane protein and the arrangement of lipid should be obtained. It contains the chromophore retinal, found elsewhere only in the visual pigments, so its light reactions have added significance in addition to having the practical benefit of occurring in a closed photochemical cycle. It is an ion pump requiring no substrates other than water and light, which nevertheless may function in principle in a general way common to other pumps involved in both ionic and molecular transport. It is found in halobacteria, which contain only a single membrane, and therefore offers the opportunity to study the induction, biosynthesis, and incorporation into the lipid bilayer of a major membrane protein. Finally, it may prove to be a useful tool in generating an electrochemical gradient for the study of the mechanism of ATP synthesis by reversible proton-translocating ATPases. It is a simple, tractable experimental system that is easy to work with and available in large quantity. Hopefully, a more complete understanding of its structure, photochemistry, and function will soon be achieved.

Literature Cited

1. Larsen, H. 1967. *Adv. Microbiol.* 1:97–132
2. Stoeckenius, W., Rowen, R. 1967. *J. Cell Biol.* 34:365–93
3. Stoeckenius, W., Kunau, W. H. 1968. *J. Cell Biol.* 38:337–57
4. McClare, C. W. F. 1967. *Nature* 216:766–71
5. Brown, A. D., Shorey, C. D. 1963. *J. Cell Biol.* 18:681–89
6. Oesterhelt, D., Stoeckenius, W. 1971. *Nature New Biol.* 233:149–52
7. Stoeckenius, W. 1976. *Sci. Am.* 234(6): 38–46
8. Blaurock, A., Stoeckenius, W. 1971. *Nature New Biol.* 233:152–55
9. Oesterhelt, D., Stoeckenius, W. 1973. *Proc. Natl. Acad. Sci. USA* 70:2853–57
10. Oesterhelt, D. 1972. *Hoppe-Seyler's Z. Physiol. Chem.* 353:1554–55
11. Oesterhelt, D., Stoeckenius, W. 1974. *Methods Enzymol.* 31:667–78
12. Oesterhelt, D. 1975. *Ciba Foundation Symp. Energy Transform. Biol. Systems* 31:147–67
13. Oesterhelt, D. 1976. *Prog. Mol. Subcell. Biol.* 4:133–66
14. Sumper, M., Reitmeier, H., Oesterhelt, D. 1976. *Angew. Chem. Int. Ed. Engl.* 15:187–94
15. Bridgen, J., Walker, I. D. 1976. *Biochemistry* 15:792–98
16. Kushwaha, S. C., Kates, M., Martin, W. G. 1975. *Can. J. Biochem.* 53: 284–92
17. Dencher, N., Wilms, M. 1975. *Biophys. Struct. Mech.* 1:259–71
18. Kushwaha, S. C., Kates, M. 1973. *Biochim. Biophys. Acta* 316:235–43
19. Kushwaha, S. C., Kates, M., Stoeckenius, W. 1976. *Biochim. Biophys. Acta* 426:703–10
20. Kates, M., Yengoyan, L. S., Sastry, P. S. 1965. *Biochim. Biophys. Acta* 98: 252–68
21. Kelly, M., Norgard, S., Liaaen-Jensen, S. 1970. *Acta Chem. Scand.* 24:2169–82
22. Dundas, J. D., Larsen, H. 1962. *Arch. Mikrobiol.* 44:233–39
23. Blaurock, A. E. 1975. *J. Mol. Biol.* 93:139–58
24. Henderson, R. 1975. *J. Mol. Biol.* 93:123–38
25. Blaurock, A. E. 1972. *Chem. Phys. Lipids* 8:285–91
26. Brown, L., Trotter, I. F. 1956. *Trans. Faraday Soc.* 52:537–48
27. Crick, F. H. C. 1953. *Acta Crystallogr.* 6:689–97
28. Pauling, L., Corey, R. B. 1953. *Nature* 171:59–61
29. Perutz, M. F. 1951. *Nature* 167: 1053–54
30. Unwin, P. N. T., Henderson, R. 1975. *J. Mol. Biol.* 94:425–40
31. Henderson, R., Unwin, P. N. T. 1975. *Nature* 257:28–32
32. Cone, R. A. 1972. *Nature New Biol.* 236:39–43
33. Razi Naqvi, K., Gonzalez-Rodriguez, J., Cherry, R. J., Chapman, D. 1973. *Nature* 245:249–51
34. Lozier, R. H., Niederberger, W. 1976. *Fed. Proc.* In press
35. Sherman, W. V., Slifkin, M. A., Caplan, S. R. 1976. *Biochim. Biophys. Acta* 423:238–48
36. Oesterhelt, D., Meentzen, M., Schuhmann, L. 1973. *Eur. J. Biochem.* 40:453–63
37. Jan, L. Y. 1975. *Vision Res.* 15:1081–86
38. Dencher, N. A., Carl, P., Sperling, W. 1976. Abstr. 10th Int. Cong. Biochem. Hamburg, p. 270
39. Oesterhelt, D., Schumann, L., Gruber, H. 1974. *FEBS Lett.* 44:257–61
40. Oesterhelt, D., Schumann, L. 1974. *FEBS Lett.* 44:262–65
41. Oesterhelt, D., Hess, B. 1973. *Eur. J. Biochem.* 37:316–26
42. Stoeckenius, W., Lozier, R. H. 1974. *J. Supramol. Struct.* 2:769–74
43. Oesterhelt, D., Hartmann, R., Fischer, U., Michel, H., Schreckenbach, T. 1975. *Proc. 10th FEBS Meet.*, pp. 239–51
44. Lozier, R. H., Bogomolni, R. A., Stoeckenius, W. 1975. *Biophys. J.* 15: 955–62
45. Chance, B., Porte, M., Hess, B., Oesterhelt, D. 1975. *Biophys. J.* 45:913–17
46. Kung, M. C., DeVault, D., Hess, B., Oesterhelt, D. 1975. *Biophys. J.* 15: 907–11
47. Sherman, W. V., Caplan, S. R. 1975. *Nature* 258:766–68
48. Kaufmann, K. J., Rentzepis, P. M., Stoeckenius, W., Lewis, A. 1976. *Biochem. Biophys. Res. Commun.* 68:1109–15
49. Lozier, R. H., Niederberger, W., Bogomolni, R. A., Hwang, S., Stoeckenius, W. 1976. *Biochim. Biophys. Acta* 440:545–56
50. Lewis, A., Spoonhower, J., Bogomolni, R. A., Lozier, R. H., Stoeckenius, W. 1974. *Proc. Natl. Acad. Sci. USA* 71:4462–66

51. Mendelsohn, R. 1973. *Nature* 243: 22–24
52. Mendelsohn, R., Verma, A. L., Bernstein, H. J., Kates, M. 1974. *Can. J. Biochem.* 52:774–81
53. Lewis, A. 1976. *Abstr. 20th Biophys. Soc. Biophys. J.* 16:204a
54. Lewis, A., Spoonhower, J. P., Perreault, G. J. 1976. *Nature* 260:675–78
55. Alfano, R. R., Yu, W., Govindjee, R., Becher, B., Ebrey, T. G. 1976. *Biophys. J.* 16:541–45
56. Hirsch, M. D., Marcus, M. A., Lewis, A., Mahr, H., Frigo, N. 1976. *Biophys. J.* In press
57. Heyn, M. P., Bauer, P.-J., Dencher, N. A. 1975. *Biochem. Biophys. Res. Commun.* 67:897–903
58. Bauer, P.-J., Dencher, N. A., Heyn, M. P. 1976. *Biophys. Struct. Mech.* 2:79–92
59. Becher, B., Ebrey, T. G. 1976. *Biochem. Biophys. Res. Commun.* 69:1–6
60. Wald, G. 1968. *Science* 162:230–39
61. Honig, B., Ebrey, T. G. 1974. *Ann. Rev. Biophys. Bioeng.* 3:151–77
62. Ebrey, T. G., Honig, B. 1975. *Q. Rev. Biophys.* 8:129–84
63. Warshel, A. 1976. *Nature* 260:679–83
64. Rosenfeld, T., Honig, B., Ottolenghi, M., Hurley, J., Ebrey, T. G. 1977. *Pure Appl. Chem.* In press
65. Thomson, A. J. 1975. *Nature* 254: 178–79
66. Salem, L., Bruckmann, P. 1975. *Nature* 258:526–28
67. Mitchell, P. 1961. *Nature* 191:144–48
68. Mitchell, P. 1966. *Biol. Rev.* 41:445–502
69. Oesterhelt, D., Krippahl, G. 1973. *FEBS Lett.* 36:72–76
70. Danon, A., Stoeckenius, W. 1974. *Proc. Natl. Acad. Sci. USA* 71:1234–38
71. Michel, H., Oesterhelt, D. 1976. *FEBS Lett.* 65:175–78
72. Bogomolni, R. A. 1976. *Fed. Proc.* In press
73. Renthal, R., Lanyi, J. K. 1976. *Biochemistry* 15:2136–43
74. Racker, E., Stoeckenius, W. 1974. *J. Biol. Chem.* 249:662–63
75. Kayushin, L. P., Skulachev, V. P. 1974. *FEBS Lett.* 39:39–42
76. Drachev, L. A., Jasaitis, A. A., Kaulen, A. D., Kondrashin, A. A., Liberman, E. A., Nemechek, I. B., Ostroumov, S. A., Semenov, A. Y., Skulachev, V. P. 1974. *Nature* 249:321–24
77. Hildebrand, E., Dencher, N. 1975. *Nature* 257:46–48
78. Bogomolni, R. A., Stoeckenius, W. 1974. *J. Supramol. Struct.* 2:775–80
79. Bogomolni, R. A., Lozier, R. H., Stoeckenius, W. 1976. *Abstr. 20th Biophys. Soc. Meet. Biophys. J.* 16:21a
80. Scholes, P., Mitchell, P. 1970. *J. Bioenerg.* 1:309–23
81. Bogomolni, R. A., Baker, R. A., Lozier, R. H., Stoeckenius, W. 1976. *Biochim. Biophys. Acta* 440:68–88
82. Lanyi, J. K., Silverman, M. P. 1972. *Can. J. Microbiol.* 18:993–95
83. Racker, E., Hinkle, P. C. 1974. *J. Membr. Biol.* 17:181–88
84. Yoshida, M., Sone, N., Hirata, H., Kagawa, Y., Takeuchi, Y., Ohno, K. 1975. *Biochem. Biophys. Res. Commun.* 67:1295–1300
85. Stoeckenius, W., Hwang, S.-B., Korenbrot, J. 1976. Nobel Symposium 34, Skovde. In press
86. Drachev, L. A., Kaulen, A. D., Ostroumov, S. A., Skulachev, V. P. 1974. *FEBS Lett.* 39:43–45
87. Berg, H. C. 1975. *Ann. Rev. Biophys. Bioeng.* 4:119–36
88. Howes, C. D., Batra, P. P. 1970. *Biochim. Biophys. Acta* 222:174–79